

Simulation Study of Underground Coal Gasification in Alberta Reservoirs: Geological Structure and Process Modeling

Hossein Nourozieh, Mohammad Kariznovi, Zhangxin Chen, and Jalal Abedi*

Department of Chemical and Petroleum Engineering, University of Calgary, 2500 University Drive, Northwest, Calgary, Alberta T2N 1N4, Canada

Received November 16, 2009. Revised Manuscript Received April 19, 2010

Underground coal gasification (UCG) as an efficient method for the conversion of the world's coal resources into energy, liquid fuels, and chemicals has attracted lots of attention in recent years. This paper is concerned with a feasibility study of the UCG process for Alberta reservoirs using the three-dimensional simulation of this process based on a unique porous media approach. The proposed approach combines the effects of heat, mass transport, and chemical reactions to achieve this goal. The Computer Modeling Group (CMG) software STARS is used for simulation. The geological structure including coal and layers interspersed between coal seams (claystone layers), the porosity/permeability variation, and the chemical processes with corresponding parameters are considered in the model. Chemical stoichiometry coefficients of the pyrolysis process are calculated from proximate and extended experimental data. Genetic algorithm and pattern search are used for parameter estimation. This model is developed to study UCG in deep coal seams and can be used for production prediction and optimization of the process. The simulation results, such as cavity formation, temperature profile, and gas composition at the producer, are presented. Finally, the results are analyzed on the basis of field pilot tests.

Introduction

Coal is a major fossil fuel in the world and plays a critical role in the energy sector. Canada is ranked 10th worldwide in coal reserves, and Alberta's 33.6 billion tons of proven mineable coal represents 70% of Canada's reserves. The deep, stranded coal reserves in Canada, which are not part of the coal reserve base, exceed 600 billion tons in Alberta alone.¹ Consequently, Alberta's coal resources constitute an enormous source of untapped energy. Therefore, there is a need for the development of novel technologies for the use of coal efficiently and cleanly. The underground coal gasification (UCG) technique can be applied to convert the abundant coal resources into a synthetic gas. The process involves the injection of steam and air or oxygen into an underground coal seam and igniting and burning of coal *in situ* to produce the combustible gas that can be used as either a fuel or a chemical feedstock. UCG has the advantages of high safety, low cost, high efficiency, environmental friendliness, and a high return rate compared to the surface gasification.² In addition, it can be applied to deep and thin coal seams that are not economic for mining.

The research goals for a recovery process are to find its potential benefits and to address the most significant issues before a field scale test. Experimental studies on UCG are time-consuming and expensive. Thus, computer modeling can

be used as an alternative to study this process. In addition, modeling can be considered as an important step for the feasibility study, design, and prediction of the process in the field scale. The UCG process involves complex physical and chemical phenomena, such as mass and heat transport, chemical reactions, and geomechanical behavior.^{3,4} For the time being, the computer modeling is the only tool to achieve a comprehensive and quantitative understanding of such a complex process.

All *in situ* gasification processes include drilling of injection and production wells into coal seams. Then, steam/oxygen or air is injected from the injector, and synthetic gases (syngas) are produced from the producer. Different techniques can be applied for a gasification process, depending upon the coal seam geological structure and technical issues involved. Two main techniques currently used by industry for UCG are linked vertical wells and controlled retracting injection points (CRIPs). The first technique requires drilling of vertical injection and production wells that are linked by a high permeable channel. This relatively old technique is suitable for thick seams and suffers from a number of operational handicaps. For instance, the burning zone and roof collapse lead to bypassing of oxygen and lowering of produced gas quality. The relatively new technique CRIP,⁵ suitable for thin, deep coal seams, replaces the vertical injector by a horizontal

*To whom correspondence should be addressed: 2500 University Dr., NW, Calgary, Alberta T2N 1N4, Canada. Telephone: 403-220-5594. E-mail: jabedi@ucalgary.ca.

(1) Energy Resources Conservation Board. Alberta's energy reserves 2007 and supply/demand outlook 2008–2017. ST98-2008, Calgary, Alberta, Canada, <http://www.ercb.ca/docs/products/sts/st98-2008.pdf> (accessed June 2008).

(2) Yang, L. H.; Yu, L.; Liang, J. Underground coal gasification in abandoned coal mines and comprehensive utility of gas products. *Coal Min. World* **1995**, 16 (1), 20–24.

(3) Yang, L.; Liu, S. Numerical simulation on heat and mass transfer in the process of underground coal gasification. *Numer. Heat Transfer, Part A* **2003**, 44 (5), 537–557.

(4) Perkins, G.; Sahajwalla, V. A mathematical model for the chemical reaction of a semi-infinite block of coal in underground coal gasification. *Energy Fuels* **2005**, 19 (4), 1679–1692.

(5) Hill, R. W.; Shannon, M. J. The controlled retracting injection point (CRIP) system: A modified stream method for *in situ* coal gasification. UCRL-85852, Lawrence Livermore National Laboratory (LLNL) Report, Berkeley, CA, 1981.

injector. During the gasification process, the burning zone grows in the upstream direction, in contrast to the gas flow in the horizontal direction. This occurs by cutting off or perforating the injection linear at successive new upstream locations. The CRIP technique produces higher quality gas, results in lower heat loss than the two-vertical well configuration, and improves the overall efficiency of the UCG process, as shown by the Rocky Mountain I (RM I) field test.⁶

UCG models of differing complexity have been reported in the literature. More complex models often give better prediction compared to simple models; however, the computational time increases considerably. Generally, two main approaches have been considered for modeling: the packed bed model and channel model. The former assumes that coal gasification occurs in highly permeable porous media with a stationary coal bed. To obtain reliable results, it is necessary to use fine grids or adaptive grid refinement in the vicinity of the front, which causes some limitation for field applications. In addition, these methods cannot clearly model the cavity growth. The latter approach assumes that, during UCG, a permeable channel or a cylindrical cavity is expanding, in which the gasification occurred in the channel or cylinder wall. These kinds of models^{7–20} were based on the one-dimensional modeling of UCG using a computational fluid dynamics

(CFD) approach. A few²¹ have considered the three-dimensional modeling of the UCG process with some assumptions, such as the absence of the heat-transfer calculation or a constant gasification temperature. A distinguishing feature of three-dimensional modeling is that the physical and chemical phenomena, such as mass and heat transport, chemical reactions, and geomechanical behavior, become far more complex.

This study considers the three-dimensional modeling of UCG using a comprehensive porous media flow approach. The model involves more than 10 chemical reactions, the main reactions that can realistically model the UCG process. These chemical processes are coupled with the mass- and heat-transfer equations. The coal seam under study is thin and deep. Therefore, the CRIP technique is appropriate and applied for the UCG modeling and prediction. The principal objectives of this work are to use the Computer Modeling Group (CMG) software STARS to carry out a feasibility study on the applicability of UCG for this coal seam in Alberta and to study reservoir and operational data that are necessary for a complete and full simulation of UCG. These data include the geological structure, chemical reaction rates, heat- and mass-transfer phenomena, thermal properties, and ignition procedure.

This paper consists of four sections: The first section considers the geological structure, porosity and permeability variation modeling, and thermal properties of seam layers. The next section provides a short description of the chemical processes occurring during UCG and the modeling of these processes. The third section reviews the governing equations for heat and mass transport followed by the model specifications and ignition procedure. Finally, results, discussions, and conclusions will be presented.

Geological Structure of Seam Layers

The geological structure of coal seams including the seam subdivision is essential for the UCG simulation study. The coal seam under study is 9 m thick and consists of nine layers. These layers have different properties, and considering all layers with very specific properties within a UCG model leads to high computational time. As estimation, all coal layers are considered to have almost the same physical properties. Similarly, all claystone layers are treated as the layers with the same properties. In addition, thin layers (either coal or claystone layers) are incorporated into other layers to ignore very thin layers within the model. Two coal layers have a thickness of less than 30 cm; therefore, they are combined with other coal layers to form three coal layers and for a total of seven layers in the coal seam. The aim of incorporating the layers is to decrease the simulation time, so that it is possible to run the field scale simulation; therefore, two sets of properties for coal and claystone layers are defined on the basis of the averaged properties of different layers. Figure 1 shows the coal and claystone layers after considering these two sets of properties for all layers. The layers interspersed between coal seams are mostly claystone with 0.5 m thickness. The overall thickness of coal layers is 7 m, and the upper subseam coal layer is the thickest (3.5 m). The average proximate analysis of the coal under study is summarized in Table 1. The coal is a highly volatile bituminous coal with a high fixed carbon content, and the interspersed layers are mostly claystone.

Porosity Calculation. The porosity of coal for different layers is unknown, and it is required for the modeling purpose.

(6) Thorsness, C. B.; Hill, R. W.; Britten, J. A. Execution and performance of the CRIP process during the Rocky Mountain I UCG field test. UCRL-98641, Lawrence Livermore National Laboratory (LLNL) Report, Berkeley, CA, 1988.

(7) Tsang, T. H. T. Modeling of heat and mass transfer during coal block gasification. Ph.D. Dissertation, University of Texas at Austin, Austin, TX, 1980.

(8) Massaquoi, J. G. M.; Riggs, J. B. Mathematical modeling of combustion and gasification of a wet coal slab—I: Model development and verification. *Chem. Eng. Sci.* **1983**, *38* (10), 1747–1756.

(9) Massaquoi, J. G. M.; Riggs, J. B. Mathematical modeling of combustion and gasification of a wet coal slab—II: Mode of combustion, steady state multiplicities and extinction. *Chem. Eng. Sci.* **1983**, *38* (10), 1757–1766.

(10) Beath, A. C.; Wendt, M.; Mallett, C. Underground coal gasification as a method for reducing the greenhouse impact of coal utilization. Proceedings of the 5th International Conference on Greenhouse Gas Control Technologies, Cairns, Queensland, Australia, Aug 13–16, 2000.

(11) Winslow, A. M. Numerical model of coal gasification in a packed bed. UCRL-77627, Lawrence Livermore National Laboratory (LLNL) Report, Berkeley, CA, 1976.

(12) Thorsness, C. B.; Grens, E. A.; Sherwood, A. A one-dimensional model for in situ coal combustion. UCRL-52523, Lawrence Livermore National Laboratory (LLNL) Report, Berkeley, CA, 1978.

(13) Abdel-Hadi, E. A. A.; Hsu, T. R. Computer modeling of fixed bed underground coal gasification using the permeation method. *J. Energy Resour. Technol.* **1987**, *109* (1), 11–20.

(14) Coeme, A.; Pirard, J.-P.; Mostade, M. Modeling of the chemical processes in a longwall face underground gasifier at great depth. *In Situ* **1993**, *17* (1), 83–104.

(15) Dinsmoor, B.; Galland, J. M.; Edgar, T. F. The modeling of cavity formation during underground coal gasification. *J. Pet. Technol.* **1978**, *30* (5), 695–704.

(16) Kreinin, E. V.; Shifrin, E. I. Mathematical modeling of the gas generation process in a coal reaction chamber. *J. Min. Sci.* **1995**, *31* (3), 230–236.

(17) van Batenburg, D. W. Heat and mass transfer during underground gasification of thin deep coal seams. Ph.D. Dissertation, Delft University of Technology, Delft, The Netherlands, 1992.

(18) Thorsness, C. B.; Cena, R. J. An underground coal gasification cavity simulator with solid motion. UCRL-89084, Lawrence Livermore National Laboratory (LLNL) Report, Berkeley, CA, 1983.

(19) Eddy, T. L.; Schwartz, S. H. A side wall burn model for cavity growth in underground coal gasification. *J. Energy Resour. Technol.* **1983**, *105* (2), 145–155.

(20) Himmelblau, D. M.; Chang, H. L.; Edgar, T. F. A sweep efficiency model for underground coal gasification. *In Situ* **1985**, *9* (2), 185–221.

(21) Biezen, E. N. J. Modeling underground coal gasification. Ph.D. Dissertation, Delft University of Technology, Delft, The Netherlands, 1996.


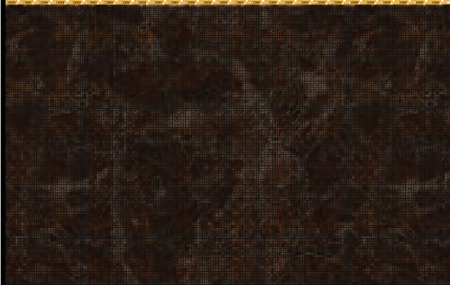





SEAM SUBVISION			
Coal Layering	Thickness [m]	Seam Name	Comment
	0.5	Roof	Claystone
	3.5	Upper Subseam	20 cm of upper subseam assigned to the middle seam
	0.5	Interspersed layer	Claystone
	1.5	Middle Subseam	
	0.5	Interspersed layer	Claystone
	2	Lower Subseam	The thickness of thin subseam added to the lower seam
	0.5	Floor	Claystone

Figure 1. Incorporated coal seam layers.

Table 1. Average Proximate Analysis for Coal and Claystone Layers

	coal	claystone
fixed carbon	55.61	4.92
volatile matter	30.36	9.05
ash	9.20	82.88
moisture	4.83	3.15

One way to calculate the coal porosity is through the bulk density, which is measured by the ultimate analysis. The assumption made here is that the known volume of coal contains ash, water, volatile, carbon, and void space (porosity). Thus, the bulk density, ash density, and pseudo-density of volatile/carbon are required to obtain the porosity of different layers.

The ash density and pseudo-density of volatile/carbon are unknown for all layers. The bulk volume consists of ash, volatile/carbon, water, and void volume. Thus

$$\text{volume} = \frac{\text{mass of ash}}{\rho_{\text{ash}}} + \frac{\text{mass of carbon + volatiles}}{\rho_{\text{pseudo}}} + \frac{\text{mass of water}}{\rho_{\text{H}_2\text{O}}} + \text{void space} \quad (1)$$

The mass of each part can be determined on the basis of 100 g of coal from a proximate analysis. For instance, the mass of ash is

$$\text{mass of ash} = \text{bulk density} \times \text{volume} \times \text{mass fraction} \quad (2)$$

The ash density and pseudo-density of volatile/carbon can be determined by eqs 1 and 2 and the results from the proximate and ultimate analyses. The generic algorithm and pattern search method are applied to obtain ρ_{ash} , ρ_{pseudo} , and void space. Table 2 summarizes the average value of void space for

Table 2. Calculated Porosity and Density for the Incorporated Layers

				density (kg/m ³)		
layer	layer number	specific gravity	bulk density (g/cm ³)	calculated porosity	volatile + carbon	ash
claystone layers	1	1.31	1.90	0.05	1596	2794
	3	1.92	2.46			
	5	1.28	2.26			
	7	2.48	2.39			
	9	2.38	2.48			
coal seam	2	1.27	1.18	0.0866	1196	2589
	4	2.43	1.28			
	6	2.27	1.14			
	8	1.28	1.22			

both coal and claystone layers, with the corresponding values for the ash density and pseudo-density of volatile/carbon.

Porosity Variation. The porosity of a grid block depends upon its solid concentration. When either pyrolysis or gasification takes place, the amount of solid inside a grid block decreases and the corresponding porosity increases. The model considered here for the variation of porosity with the solid concentration is based on the volume calculation. The current porosity is a function of the initial porosity, density, and concentration of solid inside each grid block. The previous section discussed the calculation of the averaged initial porosity and density of both coal and claystone layers.

Consider a grid block with an initial porosity of ϕ_v and solid concentration of C_s . Assuming that the solid has a pure density of ρ_s , then the current porosity is

$$\phi_{\text{fluid}} = \phi_v \left(1 - \frac{C_s}{\rho_s} \right) \quad (3)$$

This current porosity will vary with time as C_s decreases.

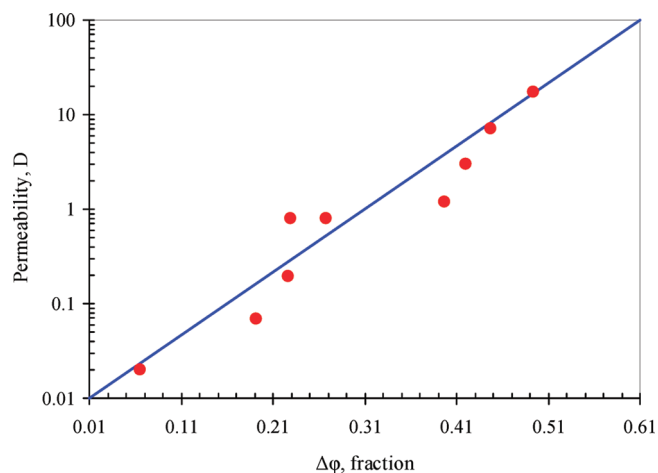


Figure 2. Permeability versus the change in porosity for the Wyodak coal during drying and pyrolysis.¹²

Permeability Variation. The permeability is a function of porosity; as the porosity increases, the permeability also increases. The published data¹² for the Wyodak coal showed that a logarithmic plot of permeability versus porosity is very nearly a linear function over the range studied. On this empirical basis, a functional relationship is

$$\ln \frac{k}{k_0} = \sigma(\phi - \phi_0) \quad (4)$$

where σ is approximately equal to 12, k_0 is the initial permeability, and ϕ_0 is the initial porosity.

Figure 2 shows the permeability variation versus porosity for the Wyodak coal in a semi-log plot.¹² The data approximately indicates a straight line. This logarithmic approach is considered in our model for the permeability variation with respect to porosity.

Thermal Properties of Layers. The thermal properties, such as thermal conductivity for different phases, must be assigned to model the heat transfer in the UCG model. The following equation is used to calculate the conductivity of each block based on various parts of the block:

$$\begin{aligned} \kappa_{\text{block}} = & (1 - \phi_v)\kappa_{\text{ash}} + (\phi_v - \phi_{\text{fluid}})\kappa_{\text{solid}} \\ & + \phi_{\text{fluid}}(S_w\kappa_w + S_g\kappa_g) \end{aligned} \quad (5)$$

The thermal properties for different layers are taken from Midttomme and Roaldset²² and given in Table 3. In eq 5, ash is defined as material that remained in the gird block after gasification.

Chemical Processes

UCG consists of drying, pyrolysis, combustion, and gasification of solid char. Figure 3 shows different regions during coal gasification *in situ*. In the first zone, which is drying (or evaporation), wet coal is converted into dry coal by increasing the temperature over 100 °C.²³ During pyrolysis, coal loses its weight, generating volatile matters and solid that is called

Table 3. Thermal Properties of Coal Seams and Claystone Layers

layer	thermal conductivity (J m ⁻¹ day ⁻¹ C ⁻¹)			
	water	gas	coal	ash
coal seam	48384	4000	2.5×10^4	2.000×10^5
claystone layers	48384	4000	2.5×10^4	2.592×10^5

char. On the basis of available experimental results, the volatile matters from the coal decompose into tar, coal gas, and chemical water. Finally, the char reacts with the injected/pyrolyzed gases to produce the syngas.

Pyrolysis. Coal pyrolysis is a chemical process in which the coal undergoes decomposition by increasing the temperature. Pyrolysis takes place when the temperature in coal is higher than the pyrolysis temperature. This process results in a series of reactions releasing volatile gases from the porous coal matrix, over the temperature range of 400–900 °C²⁴



The yields of volatiles and their composition depend upon the volatile matter content of coal, temperature, and pressure during this process. Furthermore, different gases are evolved at different temperatures during this process.²⁵ To evaluate each gas component, a kinetic model for this component is required, leading to a system of parallel reactions with different kinetic parameters.⁷ To simplify the process, pyrolysis is modeled by a simple Arrhenius expression. Therefore, the release of volatile matter is simulated as a combination of coal gases, which are evolved by increasing the temperature. Simplifying pyrolysis using a first-order chemical reaction introduces some sort of error to our model; on the other hand, using a more complicated model, more uncertain parameters (kinetic parameters) must be estimated, which can generate other errors.

Van Krevelen et al.²⁶ considered the pyrolysis process as a first-order chemical reaction

$$d\xi/dt = \varepsilon(\xi^0 - \xi) \quad (7)$$

where ξ is the volatile lost fraction of the original coal weight and ξ^0 is the effective volatile content of the coal.

The rate constant in eq 7 is typically correlated with the temperature by the Arrhenius expression

$$\varepsilon = \varepsilon_0 e^{-E/RT} \quad (8)$$

The experimental kinetic parameters for different coals are summarized elsewhere.^{27,28} Experimental data are limited to low pressure; therefore, it is necessary to extrapolate and estimate these data for high pressure.

Element Analysis of Coal Pyrolysis. In this study, the release of volatile material from coal is modeled on the basis of the following consideration: All of the major components of the volatile matter are considered, and the changes in the

(24) Anthony, D. B.; Howard, J. B. Coal devolatilization and hydrogasification. *AIChE J.* **1976**, *22* (4), 625–656.

(25) Campbell, J. H. Pyrolysis of subbituminous coal in relation to *in situ* coal gasification. *Fuel* **1978**, *57* (4), 217–224.

(26) Van Krevelen, D. W.; Van Heerden, C.; Huntjens, F. J. Physicochemical aspects of the pyrolysis of coal and related organic compounds. *Fuel* **1951**, *30*, 253–259.

(27) Nourozieh, H.; Kariznovi, M.; Chen, Z.; Abedi, J. Simulation study of underground coal gasification in deep coal seams. *Proceedings of the 8th World Congress of Chemical Engineering*, Montreal, Quebec, Canada, Aug 23–27, 2009; 0040.

(28) Kariznovi, M.; Nourozieh, H.; Abedi, J.; Chen, Z. Simulation study of underground coal gasification in Alberta reservoirs: Kinetic parameter estimation. *Fuel* **2010**, manuscript submitted.

(22) Midttomme, K.; Roaldset, E. Thermal conductivity of sedimentary rocks: Uncertainties in measurement and modelling. In *Muds and Mudstones: Physical and Fluid-Flow Properties*; Aplin, A. C., Fleet, A. J., Macquaker, J. H. S., Eds.; Geological Society of London: London, U.K., 1999; Vol. 158, pp 45–60.

(23) Lyczkowski, R. W. Mechanistic theory for drying of porous media. UCRL-52456, Lawrence Livermore National Laboratory (LLNL) Report, Berkeley, CA, 1978.

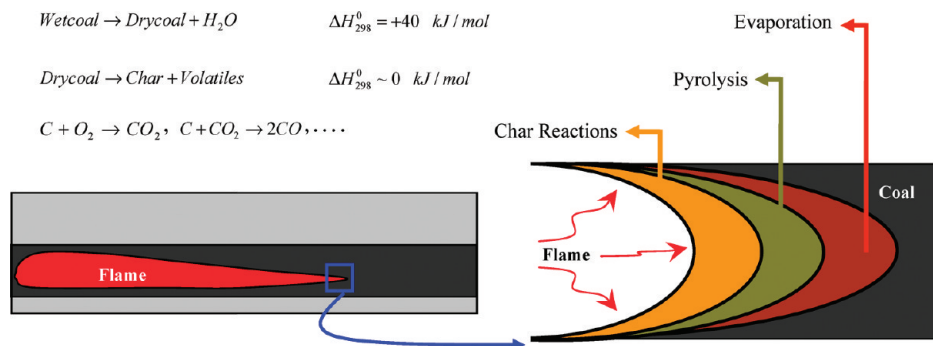
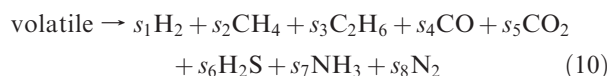
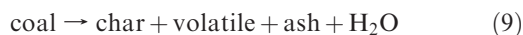


Figure 3. Different regions during UCG.

Table 4. Pyrolysis Produced Gases, Layer 1

pyrolysis produced gas (mol/100 g of coal)									ratio		
H ₂	CH ₄	C ₂ H ₆	CO	CO ₂	H ₂ S	NH ₃	N ₂	H ₂ O	CO ₂ /CO	CH ₄ /C ₂ H ₆	NH ₃ /N ₂
0.5047	0.0468	0.0468	0.2756	0.0794	0.0196	0.0104	0.0087	0.1526	0.288	1	1.191
0.5319	0.0704	0.0235	0.3218	0.0563	0.0196	0.0074	0.0102	0.1526	0.175	3	0.726
0.5700	0.0729	0.0121	0.3620	0.0362	0.0196	0.0013	0.0133	0.1526	0.1	6	0.1
0.5580	0.0844	0.0084	0.3537	0.0403	0.0196	0.0013	0.0133	0.1526	0.114	10	0.1
0.4662	0.0565	0.0565	0.2172	0.1086	0.0196	0.0036	0.0121	0.1526	0.5	1	0.295
0.4013	0.0686	0.0686	0.1448	0.1448	0.0196	0.0066	0.0106	0.1526	1	1	1.624
0.3649	0.0746	0.0746	0.1086	0.1629	0.0196	0.0107	0.0086	0.1526	1.5	1	1.255
0.3251	0.1679	0.0280	0.1086	0.1629	0.0196	0.0062	0.0108	0.1526	1.5	6	0.572
0.3002	0.1679	0.0280	0.1086	0.1629	0.0196	0.0228	0.0025	0.1526	1.5	6	9
0.5047	0.0468	0.0468	0.2756	0.0794	0.0196	0.0104	0.0087	0.1526	0.288	1	1.191

mass and composition of the solid residue are related to the release of the volatile matter by an element balance. The ash and water contents of coal are balanced directly with the proximate and ultimate analyses. The volatile matter considerably contains CH₄, C₂H₆, CO, CO₂, H₂, H₂O, NH₃, and H₂S. Indeed, these gases are a minimum number of gases required to provide a sufficiently detailed description of the volatile matter to permit reasonable accurate element balances to be constructed. In this model, the hydrocarbons heavier than ethane are considered as “ethane equivalent” and also gaseous nitrogen and sulfur components are dealt with as “ammonia equivalent” and “hydrogen sulphide equivalent”, respectively. This model is similar to the study by Merrick.²⁹ On the basis of the above consideration, the pyrolysis can be modeled by two reactions



The approach used to predict the volatile matter is to construct a set of simultaneous linear equations with the final masses of the volatile matter as unknowns

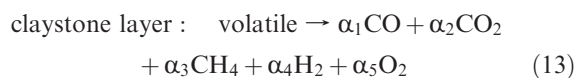
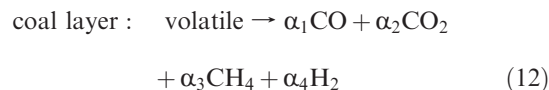
$$\sum_{j=1}^8 Q_{i,j} m_j = b_i \quad i = 1, \dots, 5 \quad (11)$$

where m_j values are the final yields of the produced gases from the coal and the values of b_i are given from the ultimate analysis of the coal. The matrix of coefficients is based on the

element balances on the carbon, hydrogen, oxygen, nitrogen, and sulfur. Three additional equations are required to have the same number of unknowns and equations. In the present study, the additional equations come from the ratios of carbon dioxide/carbon monoxide, methane/ethane, and ammonia/nitrogen.

The chemical formulation of the volatile matter and the mass of each produced gas based on the assumed produced CO₂/CO, NH₃/N₂, and CH₄/C₂H₆ ratios are listed in Table 4 for the first layer. These ratios can be found in the literature.^{25,29,30} Also, the variations of these ratios are considered to show how the produced gases are affected by these uncertain parameters. As the table shows, any change in the ratio of any produced gas has a significant effect on the amount of another produced gas.

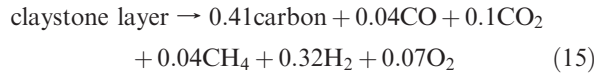
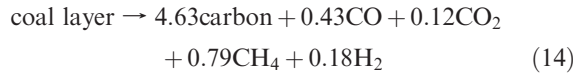
Now, on the basis of the results for different layers, two chemical reactions are assigned: one for the coal and another for the claystone layers, respectively. Because the amounts of NH₃, H₂S, and C₂H₆ are small and negligible, they will not be considered in the final equation. Sulfur and nitrogen are considered as pure components; therefore, they are eliminated from the reactions. This assumption simplifies the model and improves simulation time. The final chemical reactions to model the chemical pyrolysis for the coal and claystone layers are



(29) Merrick, D. Mathematical models of the thermal decomposition of coal: 1. The evolution of volatile matter. *Fuel* **1983**, 62 (5), 534–539.

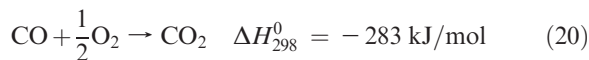
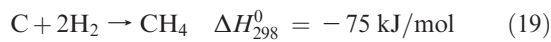
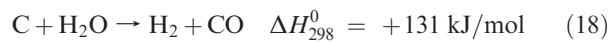
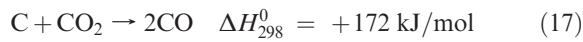
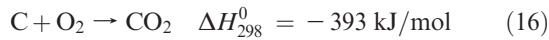
(30) Takeuchi, M.; Berkowitz, N. Fast pyrolysis of some western Canadian subbituminous coals. *Fuel* **1989**, 68 (10), 1311–1319.

The corresponding stoichiometric coefficients for the above reactions, considering char and excluding ash and water, are



The stoichiometric coefficients are obtained on the basis of the averaging of the pyrolysis process for coal and claystone layers, respectively. Contribution of each layer in the average value is determined by its thickness. That is, the thicker layer, the greater effect on the average pyrolysis gas.

Char Reactions. Char reactions are the chemical reactions among the gases within the cavity and carbon. This chemical process usually occurs after the pyrolysis is completed. The reactivity of the char to O_2 , H_2O , CO_2 , and H_2 determines the rates at which the desired products are formed. Many reactions occur during this process but the most important reactions, which are considered in the model, are summarized as follows:



Reactions 16–18 and 20 are the main chemical reactions considered for both shallow and deep coal gasification processes. The hydrogasification (reaction 19) is favorable at a high hydrogen pressure. In the UCG at low pressure, this reaction is not significant. In the presence of water, especially with low temperature, carbon monoxide–steam and methane–steam reforming reactions play an important role.

The chemical reactions are treated as the source/sink terms for each component in the model. The general heterogeneous mass-transfer reaction is defined as

$$\sum_{i=1}^n s_{i,k} B_i \xrightarrow{\varepsilon_{i,k}} \sum_{i=1}^n s'_{i,k} B_i \quad (23)$$

The kinetic model, also known as the reaction kinetics, determines the reaction speed. Its general expression is

$$r_{k,\text{chem}} = \varepsilon_{i,k} \prod_{j=1}^n C_j^{\eta_{j,k}} \quad (24)$$

In addition, the rate of creation and destruction of the i th species in reaction k is given by

$$r_{i,k} = (s'_{i,k} - s_{i,k})(\varepsilon_{i,k} \prod_{j=1}^n C_j^{\eta_{j,k}}) \quad (25)$$

Defining the net stoichiometric coefficient as $s''_{i,k} = s'_{i,k} - s_{i,k}$, the rate of creation/destruction can be written as

$$r_{i,k} = s''_{i,k} r_{k,\text{chem}} \quad (26)$$

Table 5. Chemical Kinetic Parameters as Input for Simulation²⁸

reaction	activation energy	reaction frequency factor
pyrolysis	180	2.20×10^{12}
oxidation	100	2.08×10^1
boundard	249	6.57×10^6
steam gasification	156	1.87×10^4
hydrogenation	200	1.81×10^3
carbon monoxide combustion	247	1.12×10^8
gas–steam shift forward	12.6	1.73×10^0
gas–steam shift backward	12.6	4.48×10^{-2}
methane–steam reforming forward	30.0	3.13×10^2
methane–steam reforming backward	30.0	4.00×10^3

In some cases, such as solid gasification, the term C_j in eq 25 is replaced by the partial pressure of reacting gas. The forward reaction rate $\varepsilon_{f,k}$ is assumed to have a simple Arrhenius form

$$\varepsilon_{f,k} = \varepsilon_{0,k} \exp\left(-\frac{E_k}{RT}\right) \quad (27)$$

where the activation energy E_k determines the temperature dependence of $r_{i,k}$. The chemical kinetics, which depend upon the model properties and operational conditions, were estimated and optimized at specific conditions and given in Table 5. These data were obtained on the basis of a sophisticated parameter estimation method, which is discussed in more details in the Results and Discussion.

Governing Equations

Two main transport phenomena in UCG are mass and heat physical processes. Indeed, the UCG performance and chemical process behavior are controlled by heat and mass phenomena. In the model, these conservation equations are defined in three-dimensional spaces. The convective flow for gas species inside the cavity is based on Darcy's law. For heat transport, the convection and conduction are considered as the main heat-transfer processes in the UCG model.

The mass conservation equation for component i is

$$\Delta \lambda_w y_{i,w} \Delta \varphi_w + \Delta \lambda_g y_{i,g} \Delta \varphi_g + \sum_{j=w,g} \Delta \frac{A}{\Delta l} (\rho_j D_{ij}) \Delta y_{i,j} + V \Delta (s'_{ki} - s_{ki}) r_k + q_i - \frac{V}{\Delta t} (N_i^{n+1} - N_i^n) = 0 \quad (28)$$

The first and second terms account for convective flows during the process. The third term is the mass diffusion caused by concentration variation. Mass transfer by the reaction is illustrated by the fourth term. Production and injection are considered by q_i , and finally, the last term is the accumulation term.

The transmissibility λ_j is defined as

$$\lambda_j = \left(\frac{kA}{\Delta l}\right) \left(\frac{k_{rj} \rho_j}{\mu_j}\right) \quad (29)$$

which depends upon the permeability, densities, viscosities, and grid block sizes.

For the solid components, only accumulation by combustion of solid is considered. As the pyrolysis or the char gasification takes place, the solid concentration inside the reservoir is changed. The dependence of the solid concentration upon chemical processes is given by

$$V \frac{\partial}{\partial t} [\phi_v C_i] = V \Delta (s'_{i,k} - s_{i,k}) r_k \quad (30)$$

which shows the variation of the solid with respect to time.

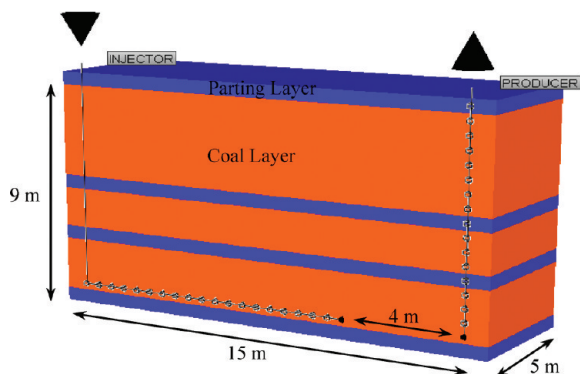


Figure 4. Model configurations, dimensions, and layering.

The energy conservation equation is

$$\begin{aligned} & \Delta \lambda_w H_w \Delta \phi_w + \Delta \lambda_g H_g \Delta \phi_g + \Delta (\kappa \Delta T) \\ & + \sum_{j=w,g} \rho_j q_j H_j + V \Delta (H_{r,k} r_k) - V \frac{\partial}{\partial t} \left\{ \phi_{\text{fluid}} \left[\sum_{j=w,g} \rho_j S_j U_j \right] \right. \\ & \left. + \phi_v C_s U_s + (1 - \phi_v) U_r \right\} = 0 \end{aligned} \quad (31)$$

The first and second terms are the flow terms of energy. Heat transport by conduction is illustrated by the third term. The well source/sink term for energy is the fourth term. The reaction source/sink term for energy is the fifth term, and the accumulation term for energy is the last term in the above equation. Here, the heat loss term is not considered; an isolated model is assumed. The transmissibility, λ_k , is defined by eq 29.

UCG Modeling

In this study, CMG's software STARS is used to carry out a feasibility study on the applicability of UCG for deep coal seams. STARS is a semi-compositional porous-media-based simulator that combines the heat- and mass-transport equations with chemical reactions to investigate the UCG process. It is a thermal and advanced processes reservoir simulator for modeling of the complex oil and gas recovery processes. This software as a commercial tool was developed to simulate the processes, such as steam flood, steam cycling, steam-assisted gravity drainage (SAGD), dry and wet combustion, along with many types of chemical processes, using a wide range of grid and porosity models in both field and laboratory scale.³¹

To simulate UCG in Alberta, the geological structure, permeability/porosity variation, and chemical reactions discussed above are taken into account in the simulator with the corresponding modeling type and parameters. As noted earlier, the coal seam under study is deep and consists of thin layers; therefore, the CRIP technique is appropriate and considered in the model. Figure 4 shows the well configuration and model dimensions. The distance between the injector toe and the producer is 4 m, and the reservoir is 15 m long, 9 m thick, and 10 m wide. It consists of three coal layers, which are identified in red color in Figure 4. The producer is just perforated in the bottom coal layer. Table 6 summarizes the seam and model properties. This model assumes that there is no heat loss or water influx from the adjacent area.

Ignition is the first step to initiate the UCG process. It consists of the following steps: First, the gas flow communication from the injector (at the open end of the well linear) to the production well is established. The permeability of the coal layers is about 1 mD, and the initial communication between the injector and producer

Table 6. Model Parameters for UCG

parameter	value
initial reservoir temperature (°C)	60
initial reservoir pressure (MPa)	11.5
coal permeability (mD)	1
claystone permeability (mD)	0.1
coal porosity, fraction	0.0866
claystone porosity, fraction	0.05
thickness (m)	9
number of coal layers	3
initial water saturation, fraction	0.7
number of grids (uniform)	10800
injected fluid	water/oxygen

is created by a fracture; therefore, a layer of high permeability that connects the injector to the producer is developed in the model. The second step is to place a coiled tubing burner in the injection well approximately 4 m back from the injector toe. The third step is to introduce O₂ to the burner tip and ignite the coal with combustible material. Finally, the O₂ injection is maintained at a minimum rate to sustain the coal burning at the injection point.

This model will be used in a sensitivity analysis and to study the effects of operating conditions on the gas composition for the coal reservoir described earlier. The operating pressure is assumed to be 11.5 MPa, and the injected oxidant is taken to be oxygen and/or water/oxygen, with a nominal oxygen injection rate of 1–3 mol/s. The variety of the water/oxygen ratio is considered to evaluate the impact of this ratio on the gas temperature and composition. The sensitivity study will be considered in more details in the Results and Discussion.

Results and Discussion

Effect of the Coal Block Size. Artifacts, such as numerical dispersion and the dependence of kinetic parameters upon the grid block size, are associated with the finite difference method used in the simulator. The former can be reduced by selecting cubic grids and a higher order finite difference (e.g., the 9-point stencil in two dimensions and the 27-point stencil in three dimensions). Here, cubic grid blocks are used for the simulation study; because of being unable to access the source code, the higher order finite difference is not used. The latter, which is more pronounced in the modeling study of heat-transfer processes, affects the modeling results even if appropriate chemical kinetics in the literature are used. In the proposed model, conversion occurs in large blocks of coal, where drying, pyrolysis, and char gasification occur simultaneously in a block; therefore, the size of coal blocks affects the behavior of the conversion process. There have been many studies about the gasification behavior of small coal particles (order of centimeters) suitable for a surface coal gasifier; however, the conversion process of large blocks of coal in UCG has not been extensively considered in laboratory studies. Two main approaches to deal with the lack of experimental data in the large blocks of coal are resizing the grid blocks or upscaling the experimental parameters.

The first approach is a proper way to eliminate the effect of the coal block size on the UCG process, but it is confined to the lab-scale physical model, where the model is less than a few meters in size. Using small grid blocks in the field scale leads to a much longer simulation time or even makes it impossible to perform a long simulation time study. Figure 5 illustrates the temperature distribution for two different grid block sizes, with the other parameters being the same. Resizing grids not only affects the temperature distribution inside the cavity but also alters the gas composition at the producer. The temperature distribution directly influences

(31) Computer Modelling Group, Ltd. <http://www.cmgl.ca/software/stars.htm>.

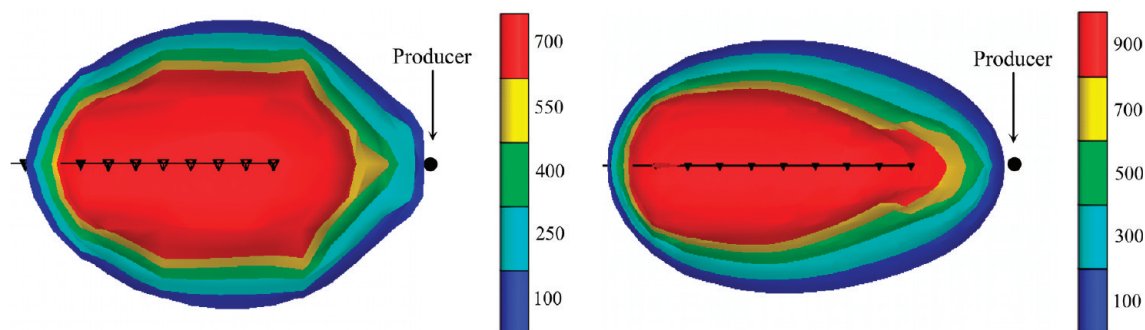


Figure 5. Effect of the coal block size on the temperature distribution: large grids (left) and small grids (right).

Table 7. Effect of the Gridblock Size on Gas Composition

gas composition (mole fraction)	CO ₂	H ₂	CO	CH ₄
grid size 0.5 × 0.5 × 0.5 m	0.3490	0.2887	0.2206	0.1416
0.25 × 0.25 × 0.25 m	0.2847	0.2557	0.2864	0.1732

chemical processes. Table 7 summarizes the gas composition for both coal block sizes.

In the second approach, which is applicable in the case of field studies, the experimental parameters (such as reaction kinetics) need to be extrapolated to be used in the simulator. This approach is used to ensure that there is proper combustion in each field-scale grid block; however, it requires field results for estimating some uncertain parameters.

Effect of the Pressure on Kinetic Parameters. The coal seam under study has an initial pressure of 11.5 MPa, but literature data on chemical reactions were reported at very low pressure. Most experiments on the chemical reactions were performed at atmospheric conditions, and there is no available data for kinetics of these reactions at higher pressure (> 11 MPa). Thus, estimation and extrapolation of experimental parameters to high pressure are essential for modeling the process.

Kinetic Parameter Estimation. As discussed before, 11 chemical processes (2 pyrolysis and 9 chemical reactions) were considered to model UCG. All of these reactions occur in UCG simultaneously and are modeled with an Arrhenius-type reaction. The chemical processes are sensitive to the coal block size and the environment conditions where the reaction occurs. Any change in the coal block size has a significant effect on the modeling results. To best represent and model UCG for the field scale, the chemical kinetics, which were obtained in the laboratory, are required to be estimated or extrapolated for field scale. From an engineering point of view, this is an inverse problem, where the aim is the determination of the model parameter(s) within a certain domain from data and information provided as final results. In UCG, the model response, which is the produced gas composition, is already known from field data, and it is necessary to estimate reaction parameters based on these results. The study by Kariznovi et al.²⁸ confirms that the Levenberg–Marquardt algorithm (LMA) can be used to investigate the uncertain parameters. The chemical kinetics (Table 5) are taken from their study, which is based on a sophisticated parameter estimation method. These data are appropriate for 11.5 MPa pressure and 0.5 m cubic coal blocks. The results based on these parameters are described in the following sections.

Cavity Shape and Temperature Profile. As a preliminary study, this work focuses on the simulation of a pilot test area

(part of the coal seam), which is 15 m long, 9 m thickness, and 10 m wide, respectively (see Figure 4). The cavity shape, temperature profile, and produced gas composition are examined here. The results illustrate the feasibility study of the UCG process for the coal seam under consideration; more future studies will be presented to investigate the effect of different operational conditions on the performance of this process. In addition, more modeling studies are required to consider the geomechanical behavior of UCG, which is not considered in this study.

Figure 6a shows the cavity shape (combustion front) after 10 days. The ignition happens at the toe of the horizontal injector, where there is a high permeability region between the wells. As the process proceeds, the injection point is perforated at successive new upstream locations. As the figure depicts, a single cavity is formed along the coal seam. The cavity grows along the *x* axis much more than along the *z* axis, which depends upon the geological structure and ignition procedure. The shale layer affects the rate of the cavity growth in the vertical direction; however, there is a vertical penetration for the gasification in the middle coal seam. In addition, the backward gasification along the *x* axis is faster than the forward gasification.

To evaluate the effect of interspersed layers (shale layers) on the cavity shape, all coal and interspersed layers are averaged into a layer with higher ash. The average permeability is calculated by

$$k_{ave} = \frac{\sum_{i=1}^7 k_i h_i}{\sum_{i=1}^7 h_i} \quad (32)$$

using the parameters given in Table 6. The cavity shape for this case is shown in Figure 6b. It clearly shows higher cavity growth in the *z* direction than the previous case, while in other directions, it is not significant. Because the geomechanic behavior is not considered in the model, it is likely that such thin interburden does not have much impact on gasification after initial linking occurs between the coal layers.

There is an area (red region) in Figure 6a where all of the coal has been affected. The corresponding cavity temperature profile is illustrated in Figure 7. The temperature inside the cavity indicates different regions during UCG. These regions are separated by lines in Figure 7. The pyrolysis region has a temperature around 500 °C during this study. This agrees with the study of Anthony and Howard,²⁴ which reported a temperature of 400–900 °C for pyrolysis during UCG.

After the pyrolysis is complete, the porous carbonaceous-rich solid referred to as char is reacted with gases inside the

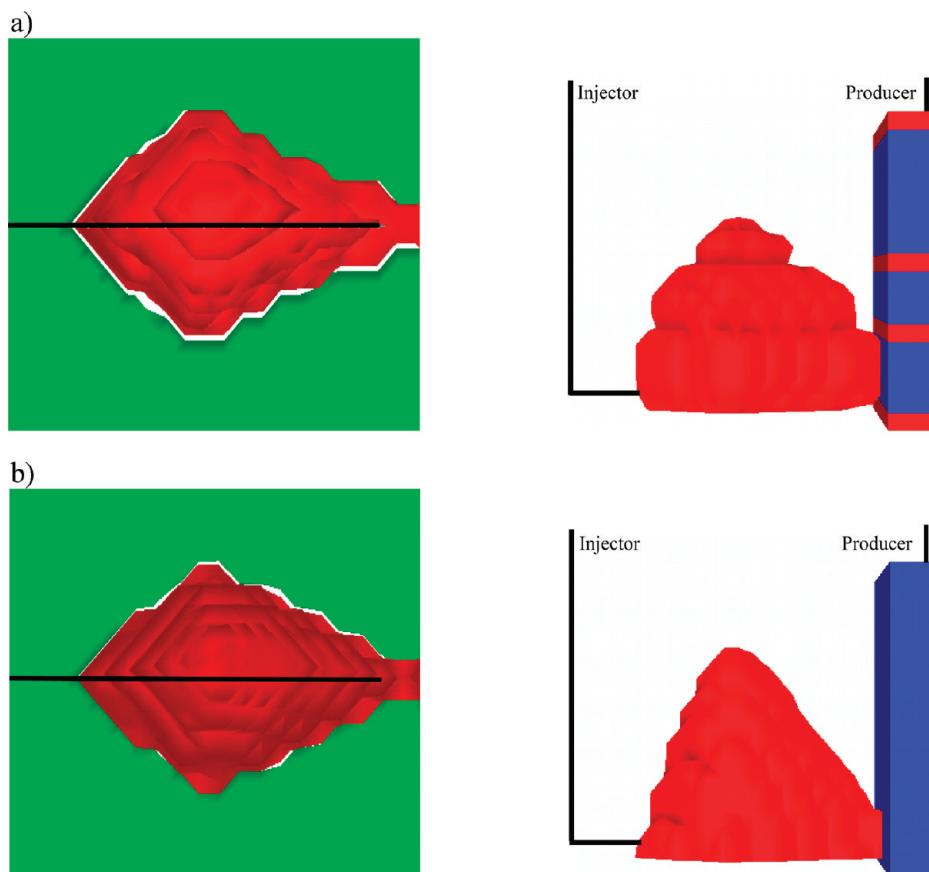


Figure 6. Cavity shape after 10 days of simulation: x - z cross (right) and x - y cross (left). (a) Corresponding to the geological structure in Figure 1. (b) Single coal layer with a higher ash content.

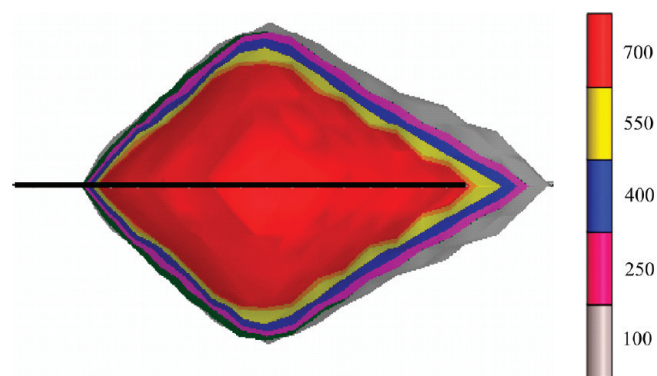


Figure 7. Cavity temperature profile (°C) after 10 days of simulation.

cavity. The temperature in Figure 7 confirms that the char gasification occurs at a temperature of around 700 °C. That is, this process happens right after the pyrolysis is complete at a temperature of 500 °C.

Sensitivity Analysis. To analyze the effect of operating conditions on the product gas composition, the operating pressure and water/oxygen ratio are taken into account. Figure 8 illustrates the variation in dry gas compositions versus the change in the water/oxygen ratio for 1 and 11.5 MPa pressures. The oxygen rate is kept at 3 mol/s constant. The increase in the methane content of the product gas at the high pressure is evident, while at lower pressure, the increase in hydrogen is expected. The former is a result of the steam methane reforming reaction, which converts carbon monoxide and hydrogen into methane and water at high pressures. This reaction leads

to a decrease in carbon monoxide and hydrogen. In addition, the reaction of carbon with hydrogen is favorable at a high hydrogen pressure. The latter is due to a higher rate of the steam gasification reaction, the reaction of water and carbon monoxide, and the low extent of the steam methane reaction at low pressure and high water concentration. At low pressure, the decrease in carbon monoxide and methane and the increase in hydrogen and carbon dioxide gas composition are reported elsewhere.^{32–34} Comparing panels a and b of Figure 8 illustrates that the gas composition is significantly affected by the pressure and water/oxygen ratio. These results give us insight into the best injection strategy to facilitate higher gas quality.

The temperature at the production well is considered as an indirect indication of the accuracy of heat-transfer calculations. For comparison, the gas temperature at the producer is summarized in Table 8. No cooling water is injected into the production well. The results show that a higher water content of injected fluid leads to a lower temperature at the producer. This can be explained by the heat absorption of the steam gasification reaction and the energy required for evaporation

(32) Hill, R. W.; Thorsness, C. B. Summary report on large block experiments in underground coal gasification, Tono Basin, Washington: Vol. 1. Experimental description and data analysis. UCRL-53305, Lawrence Livermore National Laboratory (LLNL) Report, Berkeley, CA, 1982.

(33) Yang, L. H. A review of the factors influencing the physicochemical characteristics of underground coal gasification. *Energy Sources, Part A* **2008**, 30 (11), 1038–1049.

(34) Perkins, G.; Sahajwalla, V. A numerical study of the effects of operating conditions and coal properties on cavity growth in underground coal gasification. *Energy Fuels* **2006**, 20 (2), 596–608.

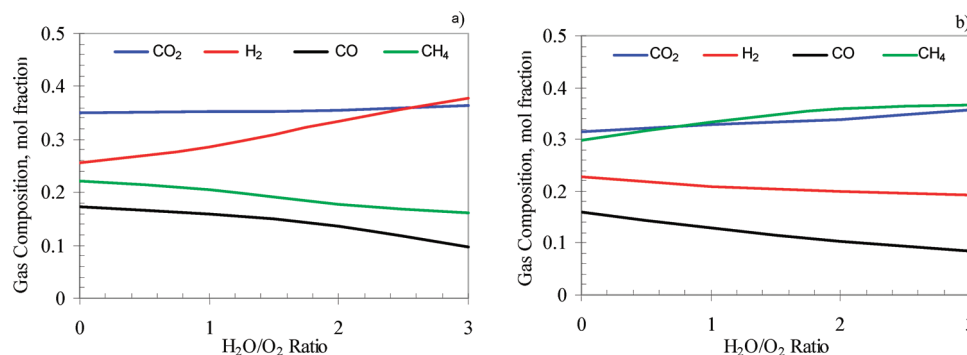


Figure 8. Effect of the water/oxygen ratio on the gas composition: (a) 1 MPa and (b) 11.5 MPa.

Table 8. Effect of the Water/Oxygen Ratio on the Gas Temperature

O ₂ rate (mol/s)	H ₂ O/O ₂ ratio			
	0	1	2	3
1	785.9	574	426	392
2	910	647.6	534.8	447.5
3	1018	797.5	650.9	571.6

Table 9. Average Gas Composition (Mole Fraction) at the Producer

	CO ₂	H ₂	CO	CH ₄
this study	0.3577	0.1850	0.0961	0.3612
European trial	0.3500	0.2500	0.1400	0.2600

of the injected water. At a constant oxygen rate, the effect of the water/oxygen ratio in the gas temperature is more pronounced at a lower ratio, and this effect becomes less evident at a higher ratio. At a constant water/oxygen ratio, the gas temperature is directly affected by the oxygen injection rate.

Table 9 gives the produced gas composition during the process. The model predicts more carbon dioxide and hydrocarbons and less synthetic gases (CO and H₂) at higher pressure than the experimental results of the European trials. The reaction of char with hydrogen is important at higher pressure, while most methane generated during the UCG process at low pressure is mainly due to the pyrolysis of coal. Also, the fraction of CO₂/CO increases as the pressure inside the gasification zone rises. The results show that, in the presence of water, the steam gasification reaction is slow, while the reaction of water and monoxide underground leads to higher hydrogen and carbon dioxide.

Conclusions and Recommendation

A three-dimensional modeling study of the UCG process using the CRIP configuration has been performed in this work. The simulation results have shown the feasibility of UCG in the coal seam under study. The proposed method for calculation of porosity and density of coal and ash has simplified the modeling of the UCG process. Considering pyrolysis as a simple reaction may result in some error to the model; however, this simplification tremendously reduces the simulation time.

The model in this study for UCG has used a porous media approach for simulation of UCG (heat and mass transfer), and the simulations have used the averaged properties of all coal and claystone layers. The simulation results have confirmed that this approach leads to accurate results. Although simplifying some parts of the process may affect the final

outcome, the results have shown that the proposed model is capable for feasibility study, design, and prediction of this process in the field scale.

On the basis of the model, the field produced gas composition for the coal under study mainly contains methane and carbon dioxide. These results are in agreement with the European field trials, where the gasification occurred at a pressure of about 5 MPa. In addition, it was found that the effect of the water/oxygen ratio on the gas composition is not the same at high and low pressures.

The geomechanical behavior of UCG is not considered in this study, but it plays an important role in this process. The geomechanical study is being investigated by our research group.

Acknowledgment. The authors acknowledge the technical support of the Computer Modeling Group (CMG), Ltd., Calgary, Alberta, Canada. Support from the Department of Chemical and Petroleum Engineering at the University of Calgary, Calgary, Alberta, Canada, and NSERC/AERI/iCORE/Foundation CMG Chair Funds is appreciated. The authors also thank two anonymous referees and Hassan Hassanzadeh for their constructive comments.

Nomenclature

A	= flow area
B	= reaction components
b	= matrix of element analysis
C	= solid concentration
D	= diffusion coefficient
E	= activation energy
H	= enthalpy
k	= permeability
k_r	= relative permeability
l	= distance
m	= matrix of final yields of produced gases
N	= number of moles
n	= number of components
Q	= matrix of coefficients
q	= injection or production rate
R	= gas constant
r	= reaction rate
S	= fluid saturation
s	= stoichiometric coefficient
T	= temperature
t	= time
U	= internal energy
V	= block volume
y	= mole fraction

UCG = underground coal gasification

CMG = Computer Modeling Group

CRIP = controlled retracting injection point

Greek Letters

ε = reaction rate constant

ϕ = porosity

φ = flow potential

η = reaction order

κ = thermal conductivity

λ = transmissibility

μ = fluid viscosity

ρ = density

σ = exponential term in permeability–porosity equation

ξ = volatile content of coal

Subscript

f = forward reaction

g = gas

s = solid

v = bulk

w = water